Carbon Chain Growth by Formyl Insertion on Rhodium and Cobalt Catalysts in Syngas Conversion**

Yong-Hui Zhao, Keju Sun, Xiufang Ma, Jinxun Liu, Dapeng Sun, Hai-Yan Su, and Wei-Xue Li*

Syngas (CO/H_2) produced from coal, natural gas, or biomass has attracted much attention as alternative to petroleum-derived fuels and chemicals. Syngas can be selectively converted to oxygenates, such as alcohols, aldehydes, and carboxylic acids, or hydrocarbons by Fischer–Tropsch synthesis (FTS).[1] Industrially, rhodium-[2] and cobalt-based[3] catalysts are often used for production of C_2 oxygenates and hydrocarbons. Despite numerous studies, the exact mechanism remains in debate, and represents a major challenge in catalysis.[4]

Formyl, formed by CO hydrogenation, has been implicated as of the key reactive intermediates in syngas conversion,[4e, 5] and it was proposed that hydrogenation of HCO followed by C=O bond scission leads to the formation of a CH_x monomer. Then chain growth proceeds by CO insertion into CH_x, by carbene coupling, or by condensation of C_1 oxygenates with elimination of water, with formation of C_n ($n \geq 2$) oxygenates or hydrocarbons. However, the short lifetime of HCO prevents its characterization, which typically requires elevated pressures, and identification of its role in syngas conversion.[6] Recently, direct evidence for HCO as the key intermediate for CO methanation was obtained by in situ spectroscopic experiments on supported Ru catalysts.[7]

Herein we report on the use of DFT calculations (for computational details, see Methods) to explore the role of HCO in syngas conversion and its dependence on the catalyst. Insertion of HCO was revealed to be an efficient alternative for chain growth on Rh(111) and Co(0001) surfaces in syngas conversion for the first time. Since HCO was proposed to be a prerequisite for the formation of a CH_x monomer (the key intermediate involved in chain growth), there should be a sufficiently high concentration of HCO for the formation of C_2 oxygenates and hydrocarbons. The results were compared to reaction pathways of CO insertion and carbene coupling. This work offers a mechanistic understanding of syngas chemistry, by achieving fundamental insight that could be used to design and develop improved catalysts for these and other important reactions of technological interest.

We first investigated competitive CO versus HCO insertion into CH_x ($x = 1$–3) on Rh(111), as shown in Figure 1a. The calculated activation energy barriers for CO insertion
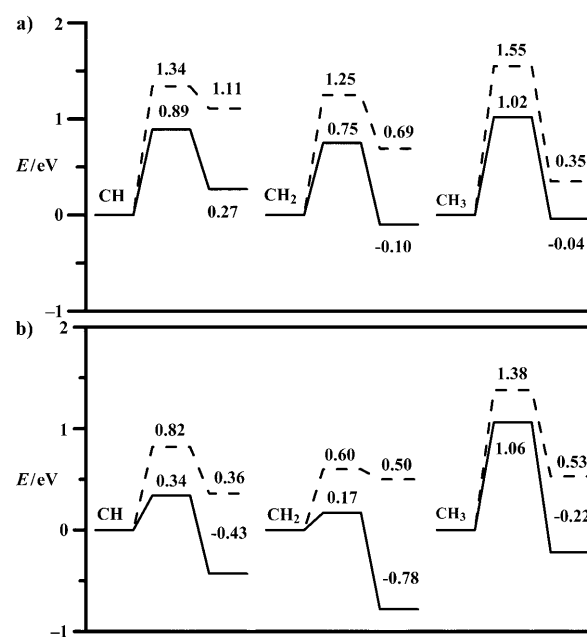
Figure 1. Calculated barriers and reaction energies for CO (dashed line) and HCO (solid line) insertion into CH_x ($x = 1$–3) on a) Rh(111) and b) Co(0001) surfaces.

into CH, CH_2, and CH_3 of 1.34, 1.25, and 1.55 eV, respectively, are significantly higher than the corresponding barriers for HCO insertion (0.89, 0.75, and 1.02 eV). Compared to the most commonly studied CO insertion pathway, the kinetic preference for the HCO insertion pathway is immediately apparent. Moreover, HCO insertion into CH_x is slightly endothermic or exothermic, with reaction energies of 0.27, −0.10, and −0.04 eV, whereas CO insertion is endothermic by 1.11, 0.69, and 0.35 eV, respectively. Therefore, the HCO insertion pathway is preferred on thermochemical grounds. Regardless of the pathway, insertion into CH_2 (CH_3) is the most kinetically favorable (unfavorable) step among all CH_x species considered. In addition, HCO dissociation into CH and O has a barrier of 1.34 eV, which is higher than those of HCO insertion into CH_x.

The preference for HCO insertion over CO insertion for CH_x can be attributed to the superior activity of HCO compared to CO (Figure 2). Compared to CO, the HOMO

[*] Y. H. Zhao, Dr. K. J. Sun, X. F. Ma, J. X. Liu, D. P. Sun, Dr. H. Y. Su, Prof. Dr. W. X. Li
State Key Laboratory of Catalysis and Center for Theoretical and Computational Chemistry, Dalian Institute of Chemical Physics Chinese Academy of Science
Zhongshanroad 457, Dalian 116023 (China)
Fax: (+86) 411-8469-4447
E-mail: wxli@dicp.ac.cn
Homepage: http://tc.dicp.ac.cn/
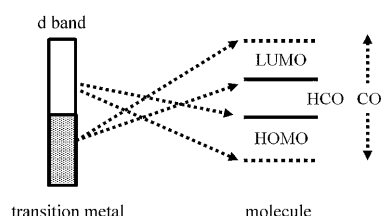
Figure 2. HUMO and LUMO of HCO (solid) and CO (dashed) and hybridization with a transition metal substrate.

level of HCO is shifted upward and the LUMO level downward, and both levels are closer to the d-band centers of transition metals. The HOMO–LUMO gap of HCO in the gas phase is 5.36 eV (5.62 eV with hybrid functional) smaller in energy than the corresponding gap for CO. The variation in HOMO and LUMO energy levels and the smaller HOMO–LUMO gap of HCO compared to CO facilitate greatly charge transfer and hybridization between HCO and catalysts. As a consequence, CO and CHO interact in completely different geometric configurations with the substrates at the transition states (TSs), as shown in Figure 3a and b, respectively, for insertion into CH_2 on Rh(111) (the initial states in Figure S1 of the Supporting Information).
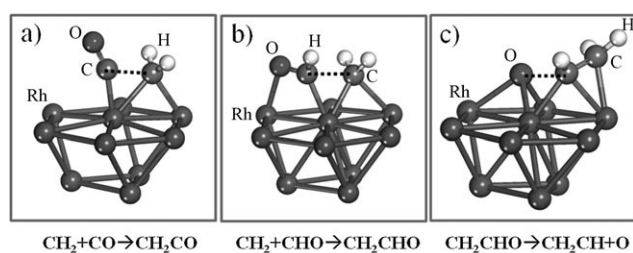
Figure 3. Structures of the optimized transition state for a) CO and b) HCO insertion into CH_2 and c) C=O bond scission of CH_2CHO on a Rh(111) surface.

For CO insertion into CH_2, CO binds through its C atom in an atop configuration, with the C–O bond tilted away from CH_2 and pointed toward the vacuum, whereas for HCO insertion, HCO has both C and O atoms coordinated to the underlying substrate, with the C–H bond pointed toward the vacuum. This configuration substantially stabilizes HCO on metal surfaces, leads to a more facile bond-making process, and thereby makes formation of oxygenates kinetically more favorable.

Previous theoretical studies focused mainly on insertion of CO into CH_x on Rh(111) with formation of oxygenates.[5f,8] However, according to our results, the HCO insertion pathway is not only energetically but also kinetically more favorable. The present calculations provide new insights into the formation of oxygenates in syngas conversion. It is of interest to compare HCO insertion and carbene coupling, which is often referred to as the most probable FTS mechanism.[9] The activation energy barriers for CH + HCO and CH_2 + HCO from this work are 0.89 and 0.75 eV, comparable to those of $CH_2 + CH_2$ (0.86–0.95 eV) and

$CH_2 + CH_3$ (0.87–1.20 eV), which have the highest activities for C–C coupling between CH_x species on Rh(111). The similar barriers for HCO insertion and carbene coupling indicate comparable selectivity for C_2 oxygenates and hydrocarbons, as is corroborated further by recent experiments on supported Rh catalysts without the presence of promoters.[4d]

We performed similar calculations for CO versus HCO insertion into CH_x on Co(0001) (Figure 1b). We find that the Co(0001) surface shows exactly the same trend as Rh(111). Kinetically, insertions of HCO into CH, CH_2, and CH_3 are easier than the corresponding CO insertion reactions by 0.48, 0.43, and 0.32 eV. Insertion of CO into CH_x is endothermic, in contrast to insertion of HCO, for which the reaction steps are downhill in energy for all CH_x species considered. A striking finding from the calculations is the rather small barriers for insertion of HCO into CH (0.34 eV) and CH_2 (0.17 eV), as opposed to 0.89 and 0.75 eV for Rh(111). This correlates with the higher reaction energies for the two reactions on Co(0001) compared to Rh(111). More specifically, the reaction energies of CH + HCO→CHHCO and CH_2 + HCO→CH_2HCO change from 0.27 eV (endothermic) and −0.10 eV (modestly exothermic) for Rh(111) to −0.43 and −0.78 eV for Co(0001), respectively. We note that the bond strength of the products CH_xHCO (Table S1, Supporting Information) is comparable on the two surfaces, with increases in adsorption energy of only 0.18 ($x = 1$) and 0.04 eV ($x = 2$). In contrast, the adsorption energy of the reactants on Co(0001) of 0.85 (CH + HCO) and 0.62 eV (CH_2 + HCO) is considerably higher than on Rh(111). Therefore, the significantly weaker adsorption of the reactants results in higher HCO insertion activity on Co(0001). The barrier for HCO dissociation into CH and O is 0.71 eV, again higher than the barriers of HCO insertion in CH and CH_2.

We are now in a position to compare HCO insertion and carbene coupling on the Co(0001) surface. It was found that chain growth by carbene coupling ($CH_2 + CH_2$) is dominant, since the insertion of CO in CH_x has significantly higher activation barriers on stepped Co surfaces.[9b,c] However, the present work suggests that even on the flat Co(0001) surface, the barriers for HCO insertion into CH and CH_2 are as low as 0.34 and 0.17 eV, which are competitive with carbene coupling. This would open a new reaction channel for chain growth on Co catalysts.

The favored reaction channels for HCO insertion into CH_x are a prerequisite for Rh, which exhibits high selectivity to oxygenates, but not necessarily for Co with high selectivity to hydrocarbons. We note that the catalytic activity for C=O bond scission in CH_xCHO is essential to address the selectivity towards oxygenates and hydrocarbons. The higher the C=O bond scission activity (lower barrier), the higher selectivity towards hydrocarbons. According to our calculations (Figure 4), Rh(111) has activation energy barriers of 1.56, 1.51, and 1.13 eV for C=O bond scission in CH_xCHO when x increases from 1 to 2 to 3, considerably higher than the corresponding barriers of 0.74, 1.21, and 0.72 eV on Co(0001). These calculations are consistent with the experimental observation that Co and Rh catalysts exhibit excellent selectivity towards hydrocarbons and oxygenates, respectively.
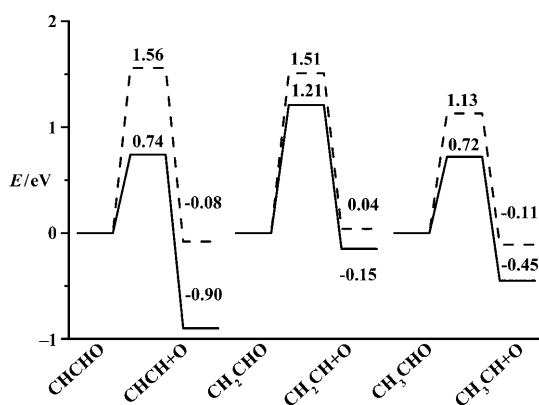
Figure 4. Calculated barriers and reaction energies for C=O bond scission of CH_xCHO (x=1–3) on Rh(111) (dashed line) and Co(0001) (solid line) surfaces.

To reveal the origin of the different activity towards C=O bond scission in CH_xCHO between Co(0001) and Rh(111), we compared carefully the TSs on the two surfaces. We found that the corresponding TSs on the two surfaces are very similar in the sense that they are late TSs. For instance, the C=O bond lengths in CH_2CHO at the TSs on Rh and Co surfaces (1.87 and 1.89 Å) are significantly elongated (Figure 3c) from the corresponding values of 1.31 and 1.36 Å at the initial states. The late TSs mean that the activation energy barriers would be largely determined by the energetics of the products, that is, O and CH_xCH. Since the binding of CH_xCH species on Co(0001) is 0.09 eV stronger (x=1) and 0.31 (x=2) and 0.32 eV (x=3) weaker than those on Rh(111) (Table S1, Supporting Information), the stronger binding of oxygen on Co(0001) compared to Rh(111) (by 0.55 eV) becomes a thermodynamic driving force for the reactions $CH_xCHO \rightarrow CH_xCH + O$ on Co(0001), as shown in Figure 4. Formation of hydrocarbons on Co is thus greatly enhanced.

Under realistic syngas conversion conditions, the presence of coadsorbed atoms/molecules on the catalysts may have a significant influence on the binding of intermediates, even for preferred reaction paths such as HCO insertion. Among them, CO is one of the most important species because it binds strongly to catalysts and acts as a spectator. Spectator CO on Co(0001) destabilizes not only CO, but also HCO in a more pronounced way.[4e] This will lead to more facile HCO insertion than CO insertion. As a result, the preference for HCO insertion over CO insertion may become even more pronounced. Quantitative investigations into the effect of coadsorbed species with extensive theoretical calculations would be desirable, but this is beyond the scope of the present work.

In summary, we have presented a DFT study on the role of formyl in syngas conversion. Insertion of HCO exhibits superior or similar activity to CO insertion and carbene coupling. This opens a new reaction channel for chain growth in syngas conversion. Cocatalysts and/or promoters with lower oxygen affinity would retard C=O bond scission (boost formyl insertion) and lead to improved selectivity for oxygenates.

Methods

All calculations were performed with the Vienna ab initio simulation package (VASP)[10] and PAW potential.[11] The wave function was expanded by plane wave with kinetic cutoff of 400 eV and density cutoff of 650 eV. The exchange-correlation energy and potential were described by generalized gradient approximation in form of the PW91[12] (hybrid functional HSE06[13] with statement explicitly) and spin-polarized calculations were performed throughout the present work. Rh(111) and Co(0001) surfaces were simulated by four-layer slabs with p(3×3) periodicity separated by a vacuum of 15 Å. The surface Brillouin zone was sampled with a (3×3×1) k-point grid by using the Monkhorst–Pack method.[14] Isolated gas-phase molecules were optimized in a (15×15.25×15.5 Å) unit cell with a single k-point. Adsorption was only allowed on one side of the slabs. The chemisorbed species and metal atoms of the top two layers were allowed to relax till the residual forces were less than $0.03\ eV\ Å^{-1}$, while the remaining atoms were fixed at their bulk truncated positions. Transition states (TSs) were located by constrained minimization and climbing-image nudged elastic band (CI-NEB) methods.[15] Various reaction pathways were explored to make sure that the lowest TSs were identified. All TSs were confirmed by frequency analysis. The reaction barriers of the elementary reaction steps were calculated with respect to the adsorbed reactants at the most stable sites with infinite separation, and zero-point vibration was not included.

[1] Q. Zhang, J. Kang, Y. Wang, *ChemCatChem* **2010**, *2*, 1030.

[2] a) S. S. C. Chuang, R. W. Stevens, R. Khatri, *Top. Catal.* **2005**, *32*, 225; b) X. Pan, Z. Fan, W. Chen, Y. Ding, H. Luo, X. Bao, *Nat. Mater.* **2007**, *6*, 507; c) N. D. Subramanian, J. Gao, X. H. Mo, J. G. Goodwin, W. Torres, J. J. Spivey, *J. Catal.* **2010**, *272*, 204.

[3] a) E. Iglesia, *Appl. Catal. A* **1997**, *161*, 59; b) S. Logdberg, M. Lualdi, S. Jaras, J. C. Walmsley, E. A. Blekkan, E. Rytter, A. Holmen, *J. Catal.* **2010**, *274*, 84; c) J. P. den Breejen, J. R. A. Sietsma, H. Friedrich, J. H. Bitter, K. P. de Jong, *J. Catal.* **2010**, *270*, 146.

[4] a) H. Schulz, *Appl. Catal. A* **1999**, *186*, 3; b) B. H. Davis, *Catal. Today* **2009**, *141*, 25; c) P. M. Maitlis, V. Zanotti, *Chem. Commun.* **2009**, 1619; d) J. Gao, X. Mo, J. G. Goodwin, *J. Catal.* **2010**, *275*, 211; e) M. Ojeda, R. Nabar, A. U. Nilekar, A. Ishikawa, M. Mavrikakis, E. Iglesia, *J. Catal.* **2010**, *272*, 287.

[5] a) H. H. Storch, N. Golumbic, R. B. Anderson, *The Fischer–Tropsch and Related Syntheses*, Wiley, New York, **1951**; b) G. P. van der Laan, A. A. C. M. Beenackers, *Appl. Catal. A* **2000**, *193*, 39; c) S. Storsæter, D. Chen, A. Holmen, *Surf. Sci.* **2006**, *600*, 2051; d) C. F. Huo, J. Ren, Y. W. Li, J. G. Wang, H. J. Jiao, *J. Catal.* **2007**, *249*, 174; e) O. R. Inderwildi, S. J. Jenkins, D. A. King, *J. Phys. Chem. C* **2008**, *112*, 1305; f) Y. Choi, P. Liu, *J. Am. Chem. Soc.* **2009**, *131*, 13054.

[6] a) W. J. Mitchell, Y. Wang, J. Xie, W. H. Weinberg, *J. Am. Chem. Soc.* **1993**, *115*, 4381; b) W. J. Mitchell, J. Xie, T. A. Jachimowski, W. H. Weinberg, *J. Am. Chem. Soc.* **1995**, *117*, 2606; c) G. A. Morgan, D. C. Sorescu, T. Zubkov, J. T. Yates, *J. Phys. Chem. B* **2004**, *108*, 3614.

[7] S. Eckle, H.-G. Anfang, R. J. r. Behm, *J. Phys. Chem. C* **2011**, *115*, 1361.

[8] a) N. Kapur, J. Hyun, B. Shan, J. B. Nicholas, K. Cho, *J. Phys. Chem. C* **2010**, *114*, 10171; b) S. Shetty, R. A. van Santen, P. A. Stevens, S. Raman, *J. Mol. Catal. A* **2010**, *330*, 73; c) D. Mei, R. Rousseau, S. M. Kathmann, V.-A. Glezakou, M. H. Engelhard, W. Jiang, C. Wang, M. A. Gerber, J. F. White, D. J. Stevens, *J. Catal.* **2010**, *271*, 325.

[9] a) J. Chen, Z.-P. Liu, *J. Am. Chem. Soc.* **2008**, *130*, 7929; b) J. Cheng, P. Hu, P. Ellis, S. French, G. Kelly, C. M. Lok, *J. Phys. Chem. C* **2008**, *112*, 6082; c) J. Cheng, P. Hu, P. Ellis, S. French, G. Kelly, C. M. Lok, *Top. Catal.* **2010**, *53*, 326.

[10] a) G. Kresse, J. Hafner, *Phys. Rev. B* **1993**, *47*, 558; b) G. Kresse, J. Furthmuller, *Phys. Rev. B* **1996**, *54*, 11169.

[11] P. E. Blochl, *Phys. Rev. B* **1994**, *50*, 17953.

[12] J. P. Perdew, K. Burke, M. Ernzerhof, *Phys. Rev. Lett.* **1996**, *77*, 3865.

[13] J. Paier, M. Marsman, K. Hummer, G. Kresse, I. C. Gerber, J. G. Angyan, *J. Chem. Phys.* **2006**, *124*, 154709.

[14] H. J. Monkhorst, J. D. Pack, *Phys. Rev. B* **1976**, *13*, 5188.

[15] a) G. Henkelman, B. P. Uberuaga, H. Jonsson, *J. Chem. Phys.* **2000**, *113*, 9901; b) G. Henkelman, H. Jonsson, *J. Chem. Phys.* **2000**, *113*, 9978.